PHYSICAL REVIEW B VOLUME 43, NUMBER 5 15 FEBRUARY 1991-I

Electronic effects in the Mo(001) surface reconstruction: Two-dimensional Fermi surfaces and nonadiabaticity

Kevin E. Smith and Stephen D. Kevan
Department of Physics, University of Oregon, Eugene, Oregon 97403
(Received 7 June 1990; revised manuscript received 2 October 1990)

The origins of the incommensurate reconstruction that Mo(001) undergoes when cooled below 220 K have been the subject of significant debate since its discovery. Much of the debate has centered on the relative importance of collective electronic phenomena in driving the reconstruction. We present here the two-dimensional Fermi surface for Mo(001), as measured using high-resolution angle-resolved photoemission spectroscopy. This Fermi surface consists of two structures: well-defined hole pockets about the $\bar{M}$ points in the surface Brillouin zone, and triangular-shaped regions midway along the $\bar{\Sigma}$ line where an electron state came very close (<0.2 eV) to E_F. These regions can be considered as Fermi-surface crossings for the purposes of coupling to surface vibrations, and thus for playing a role in driving the reconstruction. The Fermi surface is shown to support a modified version of the charge-density-wave model for the reconstruction, with the incommensurate reconstruction being pinned by nested Fermi vectors along $\bar{\Sigma}$. We discuss the role of nonadiabatic phenomena in this reconstruction, show that the electronic structure predicts that such phenomena should occur, and provide an experimental basis for the inclusion of strong electron-phonon coupling in the charge-density-wave model of the reconstruction. Finally, our results for Mo(001) are compared with our earlier results for the two-dimensional Fermi surface of W(001), and we conclude that for both surfaces a combination of Fermi-surface instabilities and strong nonadiabatic effects is the most probable driving mechanism for the surface reconstructions.

I. INTRODUCTION

The Mo(001) surface reconstructs from a commensurate (1×1) structure at room temperature to an incommensurate $c(2.2\times2.2)$ structure when cooled below 220 K.[1] The origins of this reconstruction, and the related reconstruction of W(001), have been the subject of great controversy since their first observation by low-energy electron diffraction in 1977.[1,2] Much of the debate has resulted from the existence of numerous theoretical models claiming to explain these reconstructions. Broadly defined, these models can be split into two classes, which differ according to the role collective electronic phenomena play in the surface atomic motion. The first class is known as the local bonding model, which views the reconstruction as the result of the formation of local, molecular-orbital-type, bonds at the Mo(001) and W(001) surfaces;[3–7] collective electronic effects play only a minor role. The explanation for the reconstruction of both surfaces yielded by local bonding models was widely accepted until quite recently. The second class of model is known as the charge-density-wave model, and it provided the original explanation for these reconstructions.[1,8] In this model collective phenomena dominate and the reconstructions are viewed as periodic lattice distortions resulting from potential screening anomalies produced by the spanning of heavily nested portions of the two-dimensional Fermi surface by a surface phonon wave vector.[8–11] Thus the reconstructed surface is produced by the freezing in of a particular surface phonon mode [the $\bar{M}_5$ mode in the case of W(001) and Mo(001)[2]]. The charge-density-wave model was generally discarded in favor of local bonding models following an angle-resolved photoemission measurement of the two-dimensional Fermi surface of W(001) that revealed no significant relevant nesting.[5] This occurred despite a contemporaneous photoemission study[12] of W(001) which, while not providing an independent measurement of the Fermi surface, called into doubt the accuracy of the surface state dispersion reported in Ref. 5.

Recent theoretical and experimental results have revived the debate concerning the driving mechanism for the W(001) reconstruction. Tight binding calculations of the surface phonon dispersion curves for W(001) indicate that Fermi-surface nesting, if it exists, plays a significant role in driving the reconstruction.[13] He atom scattering experiments indicate that the room-temperature W(001) surface may be slightly incommensurate and that very significant softening of surface phonon modes occurs.[14] The results of these experiments are interpreted as strong evidence for the validity of an electronic origin to the reconstruction.[14] We have recently measured the two-dimensional Fermi surface of room-temperature W(001) using high-resolution angle-resolved photoemission and found a very high density of electrons close to the Fermi level (E_F) and large-scale nesting throughout wide regions of the surface Brillouin zone.[15] This data further indicates that the charge-density-wave model may have been prematurely discarded and that collective electronic effects are likely to be of great importance in the reconstruction.

Debate concerning the origins of the Mo(001) recon-

 ©1991 The American Physical Society

struction has also intensified of late. A first principles total energy calculation and a tight binding calculation of surface phonon dispersion indicate that, as in the case of W(001), phonon mode softening would occur as a result of Fermi-surface nesting.[16] He atom scattering experiments have revealed significant phonon softening which supports an electronic driving mechanism for the reconstruction.[17] However, to date there are no published measurements of the two-dimensional Fermi surface of Mo(001).

We present here a high-resolution angle-resolved photoemission measurement of the two-dimensional Fermi surface of Mo(001) and discuss the implications of the measurement on the long running debate concerning the origins of the reconstruction. Surprisingly, this Fermi surface differs from that obtained for W(001); this is in contrast to the similarity of the Fermi surfaces obtained from Mo(011) (Ref. 18) and W(011).[19] Since the mechanism for the reconstruction of both W(001) and Mo(001) has been assumed to be identical, the measured Fermi surface will be discussed not only with regard to the Mo(001) reconstruction, but also with regard to how this measurement impacts our understanding of both surfaces. We also discuss the general concept of surface nonadiabaticity and show that both Mo(001) and W(001) have a surface electronic structure that leads to a very strong breakdown of adiabaticity, and consequently a very strong electron-phonon coupling. We consider the possibility that this leads to inherently unstable surfaces, independent of the detailed mechanism driving the reconstructions. The structure of this paper is as follows. In Sec. II the details of the experiment itself are reviewed; in Sec. III the photoemission spectra and two-dimensional Fermi surface are presented; Sec. IV contains a discussion of the Fermi-surface data and its implications, while Sec. V considers the role of nonadiabaticity in the reconstruction. The paper concludes with a summary in Sec. VI.

II. EXPERIMENT

The details of the experimental procedure and apparatus have been presented elsewhere;[18,20] only a brief review of these topics is given here. The Mo crystal was oriented using Laue x-ray diffraction and cut normal to the [001] axis. Upon introduction to the ultrahigh vacuum chamber bulk impurities (primarily carbon) were removed by repeated cycles of oxidizing at 1300 K in 1×10^{-6} Torr O_2 and flashing at 2300 K to remove the oxide. Following many hours of this treatment, Auger-electron spectroscopy revealed virtually no C or O on the surface and low-energy electron diffraction (LEED) revealed a very well ordered surface. The surface remained clean for approximately 10 min in the analysis chamber which had a base pressure of less than 1.5×10^{-10} Torr. The primary surface contaminants from the background gas were H and CO. These were easily removed by flashing the crystal to 2300 K; whatever bulk C remained in the crystal did not migrate to the surface during this procedure. Photoemission spectra were taken in two to three minutes, allowing typically two or three spectra to be accumulated before the surface required cleaning.

All experiments were performed on the beamline U4A at the National Synchrotron Light Source, Brookhaven National Laboratory. Monochromatic light was obtained using a 6-m toroidal grating monochrometer, and angle-resolved photoemission spectra were obtained using a custom designed hemispherical analyzer.[20] Typical resolution for the spectrometer in this study was less than 100 meV full width at half maximum (FWHM) and less than 1° full angular acceptance. The sample normal and azimuthal orientation were accurately determined (to less than $\frac{1}{2}$°) by using the angle-resolved photoemission analyzer to measure the spatial position of low-energy electrons diffracted from the surface.

III. RESULTS

Figure 1 shows a series of photoemission spectra obtained from clean Mo(001). The spectra were taken with 20-eV photons incident at 65° to the sample normal. The sample was oriented with the (110) mirror plane horizontal and in the plane of polarization of the synchrotron radiation. The spectra in Fig. 1 were obtained by rotating the analyzer in the plane (towards the incident light) and thus emission from states with momenta along the $\bar{\Sigma}$ line [(110) direction] in the surface Brillouin zone was detected; the surface Brillouin zone for a bcc(001) surface is shown as an inset to Fig. 1. The spectra are labeled by the momentum parallel to the surface ($k_\parallel$) of the state nearest E_F, assuming a free-electron final state.[21] The peak closest to E_F has a binding energy of approximately 0.2 eV at $k_\parallel=0$, and is very sensitive to contamination; it

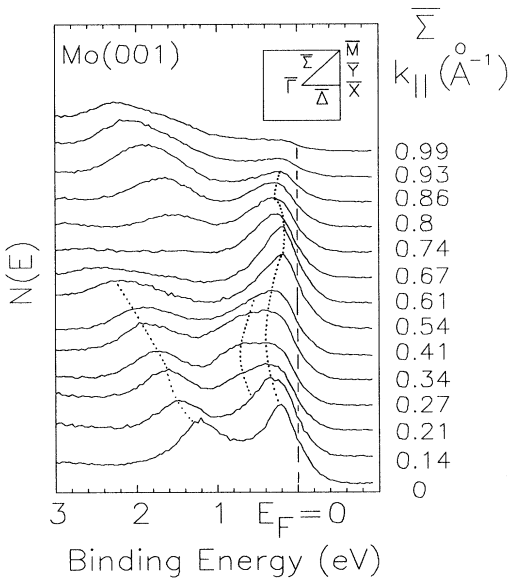

FIG. 1. A series of photoemission spectra taken from clean Mo(001) with 20-eV photons incident at 65° to the sample normal. The crystal is oriented with the (110) mirror plane in the plane of polarization of the light, and the detector is moved in the plane to measure states with $k_\parallel$ along the $\bar{\Sigma}$ direction in the zone. The surface Brillouin zone is shown as an inset.

can be completely suppressed by exposure to 1×10^{-7} Torr H_2 for 5 min. This contamination sensitivity indicates a high degree of surface localization of the electronic state being probed.[21] That the spectral feature closest to E_F in Fig. 1 indeed originates from a two-dimensional surface state (or resonance) can be further tested by measuring the binding energy of this peak as the photon energy is varied. The analyzer angle is adjusted to ensure that $k_\parallel$ remains constant, so any change in the binding energy of the peak indicates that the state has a component of momentum perpendicular to the surface, and thus is a three-dimensional state. Figure 2 shows a series of photoemission spectra from Mo(001) taken at normal emission ($k_\parallel=0$), with photons incident at 45° to the sample normal, for various photon energies. While the relative intensity of this feature varies with photon energy, the binding energy does not, further indicating the two-dimensional nature of the originating state. Although not shown, both the contamination and photon energy tests were performed on the feature at other parts of the surface Brillouin zone and the peak displayed surface characteristics throughout the zone. Note that the feature located approximately 1 eV below E_F in the normal emission spectrum of Fig. 1 does not show the same degree of contamination sensitivity and its binding energy changes with photon energy; consequently we label this feature as emission from a bulk three-dimensional state.

It is clear in the spectra of Fig. 1 that as $k_\parallel$ is increased from zero, the binding energy and width of the emission feature closest to E_F changes. In fact it is clear that between 0.1 and 0.4 Å^{-1} this peak is made up of two distinct components (both two dimensional). A similar behavior was observed for the equivalent spectra from W(001), although for W(001) the high binding energy component was resolved as a separate peak.[15] The dispersion (binding energy versus $k_\parallel$) of the surface peaks closest to E_F is shown in Fig. 3. For $k_\parallel<0.3$ Å^{-1}, the low binding energy feature disperses away from E_F slightly, reaching a maximum binding energy of 0.4 eV at 0.27 Å^{-1}. At 0.41 Å^{-1} this peak merges with the high binding energy peak, which reached its maximum binding energy of 0.75 eV at 0.2 Å^{-1}. The peak then disperses back towards E_F, reaching a binding energy of 0.2 eV at 0.54 Å^{-1}. It then remains at 0.2 eV between $k_\parallel=0.54$ and 0.61 Å^{-1}, then moves away from E_F slightly, only to disperse back and to cross above E_F at approximately 0.93 Å^{-1}. This behavior is qualitatively similar to that observed for W(001).[15] The origin of the asymmetric error bars in Fig. 3 will be discussed in Sec. IV. The dispersion curve presented here is in broad agreement with that obtained in an earlier angle-resolved photoemission study of Mo(001);[22] states with $k_\parallel$ greater than 0.5 Å^{-1} were not measured in that work.

The dispersion curve of Fig. 3 shows that there is a distinct Fermi-level crossing at 0.93 Å^{-1} along $\bar{\Sigma}$ for Mo(001). This is one point on the two-dimensional Fermi surface. In order to map out the full two-dimensional Fermi surface for Mo(001) similar dispersion curves should be measured along every direction in the surface Brillouin zone. However by taking advantage of symmetry, the full Fermi surface can be generated by measuring dispersions in only one-eighth of the zone. Figure 4 presents the measured two-dimensional Fermi surface for Mo(001). This measurement is for one-quarter of the zone, with the remaining Fermi surface generated by symmetry; frequency checks of this symmetry were performed. Nevertheless, over 1500 spectra were accumulated in this experiment. There is an acknowledged ambiguity in determining exactly where a peak crosses E_F in these photoemission spectra. However, the crossings can be determined to within approximately 0.025 Å^{-1} and any errors are systematic. Thus while the area of any

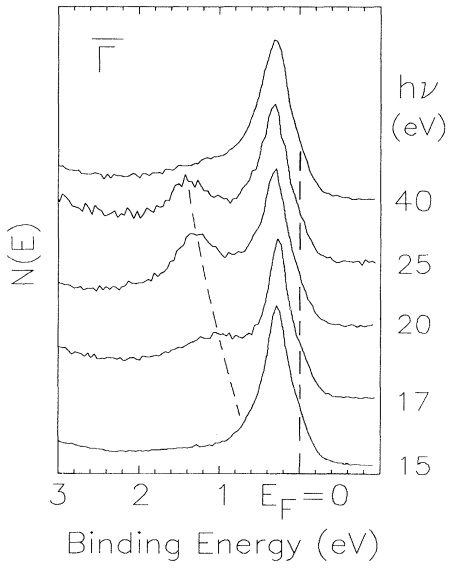

FIG. 2. A series of photoemission spectra from clean Mo(001) taken at normal emission ($k_\parallel=0$) for the photon energies indicated. The light was incident at 45°. Spectra are normalized to equal peak height to emphasize dispersion.

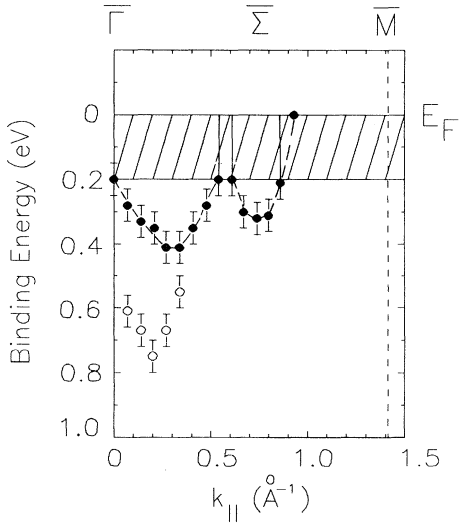

FIG. 3. Dispersion of surface states in Fig. 1. See text for details.

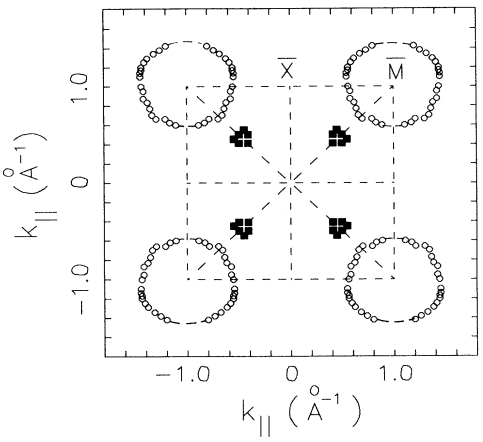

FIG. 4. Measured two-dimensional Fermi surface for Mo(001). See text for details.

features in the Fermi surface may be slightly incorrect, the shapes will not. Since one of the paramount aims of this study was to determine the *structure* of the Fermi surface, we feel the small systematic errors in the area of the Fermi-surface features to be of minor importance.

The measured two-dimensional Fermi surface for Mo(001) consists of two structures. Around the $\bar{M}$ points in the surface Brillouin zone there exist hole pockets. Similar pockets were seen for W(001).[15] However, in contrast to the case of W(001), no hole pockets were observed around $\bar{X}$. In fact for Mo(001) a well-defined surface resonance was observed at $\bar{X}$ that extended along both the $\bar{\Delta}$ and $\bar{Y}$ axes. The shaded area in Fig. 4 indicates the two-dimensional extent of the region where the surface peak is seen to come within 0.2 eV of E_F in Fig. 3. The magnitude of this structure is significantly smaller than the corresponding structure in the Fermi surface of W(001).[15]

IV. TWO-DIMENSIONAL FERMI SURFACE OF Mo(001)

The analysis of these results can conveniently be divided in two, with first a discussion of detailed structure of the measured Fermi surface of Mo(001) and how it differs from W(001), and then consideration of what role, if any, this Fermi surface could play in driving the M(001) reconstruction.

A. Fermi-surface structure

The Fermi surface for a free electron gas can be defined as the surface in k space that, at zero temperature, encloses all the occupied electronic states. In a solid where the one-electron-band picture is a reasonable approximation to reality, the Fermi surface is thus defined by the surface that connects in k space all the points where electron bands cross E_F. Since angle-resolved photoemission spectroscopy in principle allows one-electron-band dispersions to be directly measured, the determination of the Fermi surface using photoemission is, in theory, trivial. Due to inescapable ambiguities in determining the exact point in k space at which a photoemission peak crosses E_F, the accuracy attained in measuring three-dimensional Fermi surfaces using photoemission is significantly less than that achieved with other methods (for example, the de Haas–van Alphen effect). However, magnetic techniques or positron annihilation have very great difficulty in determining two-dimensional Fermi surfaces at all. Since angle-resolved photoemission can easily distinguish between two- and three-dimensional states, this has become the only routine method for determining the structure of two-dimensional Fermi surfaces.

As is clear from the data in Fig. 1, and as is illustrated in Fig. 3, there is an unambiguous disappearance of a photoemission peak across E_F at approximately 0.93 Å^{-1} along $\bar{\Sigma}$. By moving the detector off the $\bar{\Delta}$ axis, the behavior off this peak at other points in the zone can be monitored. The resulting Fermi-surface structures defined by the crossing of this state above E_F are the hole pockets around the $\bar{M}$ points in the surface Brillouin zone shown in Fig. 4. This peak is seen in the photoemission spectra when the detector is swept both in the plane of polarization and perpendicular to it, although the hole pocket structure was most easily determined moving the detector out of plane. This indicates that the state is of mixed symmetry with respect to the (011) mirror plane,[23] with the odd component most visible moving the detector out of plane. This in turn indicates a significant, though far from exclusive, $d_{x^2-y^2}$ orbital character to the peak in this region. This kind of loose identification of a one-electron d band with a molecular d orbital of particular mirror plane symmetry is only possible in the absence of significant spin-orbit coupling, as is the case for Mo. Nonrelativistic tight binding calculations for Mo(001) (Refs. 16, 24, and 25) predict a state of $d_{x^2-y^2}$ character to cross E_F at approximately 0.9 Å^{-1} along $\bar{\Sigma}$, in agreement with where we observe a peak to cross E_F. [Similar nonrelativistic calculations for W(001) have much less success reproducing the measured band dispersions near $\bar{M}$ (Ref. 15).] Additionally, the projected bulk band structure shows an absolute band gap at E_F from 0.53 to 1.11 Å^{-1} along $\bar{\Sigma}$.[24] Thus in this region the photoemission peak can be associated with a surface state rather than a surface resonance.[21]

Entirely absent from the two-dimensional Fermi surface presented in Fig. 4 are any hole pockets around the $\bar{X}$ point in the surface Brillouin zone. In fact, a well defined surface resonance could be detected about 0.45 eV below E_F around $\bar{X}$. [A detailed analysis of the experimentally determined two-dimensional band structure of Mo(001), as distinct from the two-dimensional Fermi surface, is presented elsewhere.[26]] The absence of these $\bar{X}$ hole pockets is quite surprising. It was considered a general phenomenon that many regions of two-dimensional Fermi surfaces mimicked projections of bulk, three-dimensional Fermi surfaces onto the appropriate plane. This has been observed for the ellipsoidal hole structures on W(001) (Ref. 15), W(011) (Ref. 19), and Mo(011),[18] and is interpreted as a reluctance on the part of the surface resonances to cross the boundary between the occupied projected bulk states into a projected bulk band gap. A projection of the measured bulk Fermi surface of Mo[27] gives hole pockets at both $\bar{M}$ and $\bar{X}$, and thus the lack of

a measured two-dimensional hole pocket at $\bar{X}$ indicates a state to resonance transition in this region.[26] [The projected bulk Fermi surface for W(001) is provided in Ref. 15; the bulk Fermi surfaces of Mo and W are quite similar and likewise the projections.] Note that the measured hole pockets about $\bar{M}$ have a larger area on Mo(001) than on W(001).[15] This is to be expected since the hole ellipsoids in the measured bulk Fermi surface that project onto the $\bar{M}$ point are larger in Mo (Ref. 27) than in W.[28]

Aside from the hole pockets about $\bar{M}$, the Fermi surface (Fig. 4) displays only one other feature: the small triangular structures located towards the midpoint of the $\bar{\Sigma}$ lines. The data points defining these structures require some explanation, since in rigorous terms they are not legitimate Fermi-surface crossings and as such must be distinguished from the $\bar{M}$ hole pocket data points. The dispersion curve in Fig. 3 reveals that after initially dispersing away from E_F as $k_\parallel$ is increased from zero along $\bar{\Sigma}$, the low binding energy state disperses towards E_F for $k_\parallel > 0.34$ Å^{-1}, reaching its point of closest approach to E_F at $k_\parallel = 0.54$ Å^{-1}. At this point in k space the binding energy of the peak in the photoemission spectrum is determined to be 0.2 eV (Fig. 1). However, the peak shows no sign of crossing E_F and remains at 0.2 eV until $k_\parallel = 0.61$ Å^{-1}, at which point it begins to disperse away from E_F. The data points in the Fermi surface of Fig. 4 that make up the triangular structures are the limiting points of the region in k space where this state has a binding energy of 0.2 eV. The reason for including these points in the Fermi surface is the following. Photoemission peaks have an inherent width that has origins both in the electronic properties of the material being probed and in the photoemission process itself.[21] Determining the binding energy of an electron state in a metal is not, however, a problem until the state approaches E_F. Once close to E_F, the convolution of the linewidth function for the peak and the Fermi function at E_F introduce an uncertainty in determining the exact binding energy of the state with respect to E_F. There is, in fact, a possibility that the state in question here is considerably closer to E_F than 0.2 eV, and may even be at E_F. Consequently, the entire triangular structure can be viewed as points where a surface state "crosses" E_F. (Hence the asymmetric error bars and shaded threshold region in Fig. 3.) Even without crossing E_F, the generalized susceptibility will be strongly influenced by states this close to E_F. A similar type of structure was observed in the Fermi surface of W(001), although of much larger extent.[15] It must be stressed that the choice of 0.2 eV as the binding energy at which this ambiguity in the state energy becomes significant is arbitrary. Clearly with the resolution of our spectrometer, there is little error for example in assigning a state energy of 1 eV to a spectral feature at 1 eV. However, deciding at what smaller binding energy the ambiguity becomes significant is subjective. It would not be unreasonable to set the cutoff at 0.3 eV, in which case almost half the area of the zone would be included in the shaded structures (see Fig. 3). The relevance of this measured Fermi surface for the debate concerning the driving mechanism for the Mo(001) reconstruction will now be considered.

B. Fermi surfaces and reconstruction

The charge-density-wave model, which regards the reconstruction of a surface as a periodic lattice distortion, is very attractive from an experimental point of view. The basic physics underlying a periodic lattice distortion is the existence of a large potential screening anomaly (susceptibility anomaly) caused by the spanning of heavily nested regions of the Fermi surface by the wave vector of a lattice vibration.[29] Without a heavily nested Fermi surface (i.e., a Fermi surface that contains large flat parallel segments) a periodic lattice distortion cannot occur. (The converse is not true, however; the observation of a nested Fermi surface does not alone guarantee the occurence of a periodic lattice distortion.) In any event, if the two-dimensional Fermi surface can be measured for a surface that undergoes reconstruction, then the validity of the charge-density-wave model can be immediately revealed. As was noted above, it was just such a measurement of the Fermi surface of W(001) that led to the original demise of this model as an explanation the W(001) reconstruction.[5] This dismissal of a collective electronic origin to the W(001) reconstruction has had to be reconsidered in the light of recent He atom scattering experiments[14] and our recent W(001) Fermi-surface measurement.[15]

The validity of the charge-density-wave model as an explanation for the Mo(001) reconstruction has, until now, never been directly tested by measuring the Mo(001) two-dimensional Fermi surface. LEED indicates that the wave vector of the displacements on Mo(001) is approximately 0.91 $(\pi/a, \pi/a)$, i.e., 1.29 Å^{-1} along $\bar{\Sigma}$.[1] Thus the classic charge-density-wave model requires that there be flat segments of Fermi surface perpendicular to the (110) direction, separated by 1.29 Å^{-1}. Consider first the $\bar{M}$ hole pockets in the Fermi surface of Fig. 4. There are two possible nesting vectors along $\bar{\Sigma}$, and these can only be considered as nested if the curvature of the hole pockets close to $\bar{\Sigma}$ is judged to be insignificant. The first nesting vector is just $2k_F$, i.e., the vector from the Fermi-level crossing along $\bar{\Sigma}$ closest to $\bar{\Gamma}$ on one side of the first zone, to the equivalent point on the other side of the zone along $\bar{\Sigma}$. The magnitude of this vector is 1.86 Å^{-1} and thus this nesting vector has little in driving the reconstruction. The second nesting vector associated with the $\bar{M}$ hole pocket is the vector along $\bar{\Sigma}$ that spans the pocket itself. The expression for this vector is $G - 2k_F$, where G is a surface reciprocal lattice vector, and its magnitude is 0.97 Å^{-1}. Thus this nesting vector also fails to satisfy the requirements of the classic CDW model to explain the observed reconstruction.

There remains another set of nesting vectors in the measured Fermi surface (Fig. 4) that have not yet been considered. These are the vectors associated with the triangular structures along $\bar{\Sigma}$. If the obvious lack of large segments perpendicular to $\bar{\Sigma}$ is neglected momentarily, then the vector connecting the centers of these structures across the zone center ($2k_F$) is 1.15-Å^{-1} long. If k_F is taken as the vector extending to the flat segment furthest from $\bar{\Gamma}$ (the base of the triangle), then $2k_F$ becomes 1.22 Å^{-1}. These vectors are very close in magnitude to the displacement vectors observed in the LEED experiment.[1]

Thus the Fermi-surface vectors associated with the triangular structures satisfy part of the requirements of the classic charge-density-wave model. It is unclear what effect the lack of a large extent to these structures perpendicular to $\bar{\Sigma}$ has on the bare susceptibility. If the nesting vector to the base of the triangle is used, the perpendicular extent is over 0.2 Å^{-1}, which is probably sufficient to drive the screening singular. As noted above, the cutoff of 0.2 eV used to define these structures is arbitrary, and were, for example, a threshold of 0.3 eV used, then the extent of these structures would be much larger. Of course if this threshold is chosen, then a much larger number of wave vectors will span the Fermi surface (from 1 to 1.86 Å^{-1}). The full significance of the existence of these triangular Fermi surface structures will only become apparent when the role of nonadiabaticity in the reconstruction is considered below.

The use of these nonstandard Fermi-surface structures in the charge-density-wave model comes with a significant caveat. It must be emphasized that no crossing of a photoemission feature above E_F is seen in the spectra (Fig. 1) in these triangular regions. Thus they do not denote conventional Fermi-surface crossings. What is seen is a photoemission peak that approaches the Fermi level to a binding energy equivalent to its natural linewidth. This means there is a finite possibility that the related one-electron state is at E_F. Additionally, nested states this close to E_F will have a significant impact on the susceptibility even if they do not cross E_F. These are sufficient justifications for including these structures in the Fermi surface, and for considering their possible role in the charge-density-wave model.

Thus far the focus of attention has been on the classic charge-density-wave model for surface reconstruction as originally proposed by Tossatti.[8] Modifications of the Fermi-surface model have been proposed for both bulk Kohn anomalies in Mo (Ref. 30) and for the Mo(001) reconstruction.[16] The primary change in the model is greater consideration of the role of electron-phonon coupling in modifying the behavior of the generalized susceptibility. It has recently been shown that inclusion of electron-phonon matrix effects into the charge-density-wave model results in a prediction of maximum phonon instability at a phonon wave vector of 1.17 Å^{-1} along $\bar{\Sigma}$ (Ref. 16). Significantly, a recent He atom scattering experiment where the surface phonon mode dispersion was directly measured,[17] found the $\bar{M}_5$ phonon mode to go to zero at approximately 1.1 Å^{-1}, not 1.29 Å^{-1} as expected from the LEED analysis.[1] Our observation of nested states close to, or at, E_F in this region of the surface Brillouin zone lends further credibility to this model. Note that although a nesting vector of 0.97 Å^{-1} is observed across the $\bar{M}$ hole pocket, the associated band is dispersing rapidly, leading to only a small two-dimensional density of states (DOS) for this state. The role of this vector is considered to be less significant than that associated with the triangular structures (with a wave vector of 1.08 to 1.22 Å^{-1}) due to their much larger DOS.

V. NONADIABATICITY AND THE INHERENT INSTABILITY OF Mo(001) and W(001)

The addition of explicit electron-phonon coupling effects into the charge-density-wave model produces a theory[16] that predicts the results of the He atom scattering experiment,[17] and is consistent with the two-dimensional Fermi surface presented here. Electron-phonon coupling can be viewed as a direct manifestation of the breakdown of the adiabatic approximation in a solid. In this approximation, the motion of atoms and electrons in a solid are considered to be completely independent.[31] This is often a valid approximation because electron velocities are far larger than atom velocities in most solids. However, the adiabatic approximation will break down if the velocity of electrons (or summed velocity of pairs of electrons) is reduced. If we neglect the case of paired electrons, then in a one-electron band picture the requirement of slow electrons translates as a need for flat, nondispersive bands. Additionally, since phonon vibrational energies are typically much smaller than electron binding energies, a strong breakdown of adiabaticity will only occur if flat electron bands reside close to E_F. Electrons in flat, nondispersive bands near E_F have been shown to play a fundamental role in the damping of certain adsorbate vibrations on surfaces.[32–34] In this section we wish to discuss in general terms how the electronic structure we measure for both Mo(001) and W(001) leads to strong nonadiabatic effects, and is ultimately responsible for the inherent instability of both surfaces towards reconstruction.

Using photoemission spectroscopy we have found that both Mo(001) and W(001) (Ref. 15) have two-dimensional bands that are nondispersive very close to E_F over significant regions of the surface Brillouin zone. (Figure 3 shows the shallowest band along $\bar{\Sigma}$ to have a width of less than 0.4 eV.) Consequently, there is a very high two-dimensional DOS close to E_F in these regions. Thus, with both a high density of states and slow electrons in flat bands at E_F, strong nonadiabatic effects are inevitable. Indeed, nonadiabatic adsorbate vibrational damping has been observed using infrared spectroscopy for hydrogen atoms adsorbed on both Mo(001) (Ref. 35) and W(001).[33] We believe nonadiabatic damping of intrinsic surface vibrations (i.e., strong electron-phonon coupling) also must occur at both Mo(001) and W(001) surfaces. This would imply that these surfaces are inherently unstable to reconstruction, since with strong electron-phonon coupling it is logical to assume that the energy of electrons at E_F can be reduced by many lattice distortions, and thus many lattice distortions (reconstructions) are energetically favorable.

The argument that nonadiabatic effects lead to surfaces that are unstable to arbitrary displacements has been considered in a number of theories.[3,4] These theories have usually viewed this as pointing towards a localized mechanism for the reconstructions. However, we believe the electronic structure data we have obtained indicates that

the reconstruction of both Mo(001) and W(001) is a result of a strong interplay between nonadiabatic and Fermi-surface phenomena. We come to this conclusion by the observation on both surfaces of an electronic structure that contains appropriately nested two-dimensional Fermi surfaces *and* a high density of nonadiabatic electrons. This idea is in essence the same as that underlying the theory of Wang *et al.* for the Mo(001) reconstruction.[16] That theory was shown above to be compatible with our measured Mo(001) Fermi surface. However, strong electron-phonon coupling plays a major role in this theory,[16] and our measurements predict that such a strong breakdown of adiabaticity should occur. Furthermore, in considering the nonadiabatic vibrational damping of H on W(001), we formulated a set of selection rules for the effective nonadiabatic coupling of a vibrational mode to an electronic state.[34] One of these states that the product of the initial and final electronic state and the vibrational mode symmetries should be even with respect to some mirror plane of the surface. If we consider the (110) mirror plane, then the $\bar{M}_5$ phonon mode is of odd symmetry. The triangular structures in the Fermi surface lie in a region of k space where only even bulk states exist close above E_F in the projected bulk band structure.[24] Thus the available final electronic states are of even symmetry. Consequently, we would predict strong nonadiabatic coupling of a surface state to the $\bar{M}_5$ phonon mode only if that state were of odd symmetry. As noted in Sec. IV, the band that forms both the triangular structures and the M hole pockets in the Fermi surface is of mixed symmetry with respect to the (110) plane, and thus this coupling is allowed.

VI. SUMMARY

We have presented here the two-dimensional Fermi surface for Mo(001), as measured using high-resolution angle-resolved photoemission spectroscopy. This Fermi surface consists of two structures: well-defined hole pockets about the $\bar{M}$ points in the surface Brillouin zone, and triangular-shaped regions midway along the $\bar{\Sigma}$ line where an electron state came very close (<0.2 eV) but did not cross E_F. We consider that this state is close enough to E_F in these triangular regions that these regions can be considered as true Fermi-surface crossings for the purposes of coupling to surface vibrations, and thus for playing a role in driving the reconstruction. The Fermi surface was shown to support the charge-density-wave model for the reconstruction by Wang *et al.* [16] with the incommensurate reconstruction being pinned by nested Fermi vectors along $\bar{\Sigma}$. We discussed the role of nonadiabatic phenomena in this reconstruction, showed that the measured electronic structure predicts that such phenomena should occur, and provided an experimental basis for the inclusion of strong electron-phonon coupling in the Fermi-surface model of Wang *et al.* [16] Finally, our results for Mo(001) were compared throughout with our earlier determination of the two-dimensional Fermi surface of W(001), and we conclude that for both surfaces a combination of the conventional charge-density-wave model of Tossatti[8] and strong nonadiabatic effects drives the surface reconstructions.

ACKNOWLEDGMENTS

This work was supported in part by U.S. Department of Energy (DOE) Grant No. DE-FG06-86ER45275, and undertaken at the National Synchrotron Light Source, Brookhaven National Laboratory, which is supported by the U.S. DOE, Divisions of Materials Sciences and Chemical Sciences. S.D.K. would like to acknowledge the National Science Foundation and the A. P. Sloan Foundation for financial support.

[1]T. E. Felter, R. A. Barker, and P. J. Estrup, Phys. Rev. Lett. **38**, 1138 (1977); R. A. Barker, S. Semancik, and P. J. Estrup, Surf. Sci. **94**, L162 (1980).

[2]M. K. Debe and D. A. King, Phys. Rev. Lett. **39**, 708 (1977); Surf. Sci. **81**, 193 (1979).

[3]J. E. Inglesfield, J. Phys. C **12**, 149 (1979).

[4]K. Terakura, I. Terakura, and Y. Teraoka, Surf. Sci. **86**, 535 (1979); I. Terakura, K. Terakura, and N. Hamada, Surf. Sci. **103**, 103 (1981); **111**, 479 (1981).

[5]J. C. Campuzano, J. E. Inglesfield, D. A. King, and C. Somerton, J. Phys. C. **14**, 3099 (1981); D. A. King, Phys. Scr. **T4**, 34 (1983).

[6]D. Singh and H. Krakauer, Phys. Rev. B **37**, 3999 (1988).

[7]V. Heine and J. J. A. Shaw, Surf. Sci. **193**, 153 (1988).

[8]E. Tossatti, Solid State Commun. **25**, 637 (1978).

[9]J. C. Campuzano, D. A. King, C. Somerton, and J. E. Inglesfield, Phys. Rev. Lett. **45**, 1649 (1980).

[10]J. E. Inglesfield, J. Phys. C. **11**, L69 (1978).

[11]H. Krakauer, M. Posternak, and A. J. Freeman, Phys. Rev. Lett. **43**, 1885 (1979).

[12]M. I. Holmes and T. Gustafsson, Phys. Rev. Lett. **47**, 443 (1981).

[13]X. W. Wang and W. Weber, Phys. Rev. Lett. **58**, 1452 (1987).

[14]H. J. Ernst, E. Hulpke and J. P. Toennies, Phys. Rev. Lett. **58**, 1941 (1987); Europhys. Lett. **10**, 747 (1989); B. Salanon and J. Lapujoulade, Surf. Sci. **173**, L613 (1983).

[15]K. E. Smith, G. S. Elliott, and S. D. Kevan, Phys. Rev. B **42**, 5385 (1990); G. S. Elliott, K. E. Smith, and S. D. Kevan (unpublished).

[16]X. W. Wang, C. T. Chan, K. M. Ho, and W. Weber, Phys. Rev. Lett. **60**, 2066 (1988).

[17]E. Hulpke and D. M. Smilgies (unpublished).

[18]K. Jeong, R. H. Gaylord, and S. D. Kevan, Phys. Rev. B **39**, 2975 (1989).

[19]R. H. Gaylord, K. Jeong, and S. D. Kevan, Phys. Rev. Lett. **62**, 2036 (1989); R. H. Gaylord, K. Jeong, S. Dhar, and S. D. Kevan, J. Vac. Sci. Technol A **7**, 2203 (1989).

[20]S. D. Kevan, Rev. Sci. Instrum. **54**, 1441 (1983).

[21]For a discussion of the principles of band determination using angle resolved photoemission, see E. W. Plummer and W. Eberhardt, Adv. Chem. Phys. **49**, 533 (1982).

[22]S. L. Weng, E. W. Plummer, and T. Gustafsson, Phys. Rev. B **18**, 1718 (1978).

[23]J. Anderson, G. J. Lapeyre, and R. J. Smith, Phys. Rev. B **17**,

2436 (1978).
[24]C. M. Bertoni, C. Calandra, and F. Manghi, Solid State Commun. **23**, 255 (1977).
[25]P. C. Stephenson and D. W. Bullett, Surf. Sci. **139**, 1 (1984).
[26]K. E. Smith and S. D. Kevan (unpublished).
[27]D. M. Sparlin and J. A. Marcus, Phys. Rev. **144**, 484 (1966).
[28]R. F. Girvan, A. V. Gold, and R. A. Phillips, J. Phys. Chem. Solids **29**, 1485 (1968).
[29]See, for example, S. K. Chan and V. Heine, J. Phys. F **3**, 795 (1973).
[30]C. M. Varma and W. Weber, Phys. Rev. B **19**, 6142 (1979).
[31]N. W. Ashcroft and N. D. Mermin, *Solid State Physics* (Saunders College, Philadelphia, 1976).
[32]Z. Y. Zhang and D. C. Langreth, Phys. Rev. B **39**, 10028 (1989) and references therein.
[33]Y. Chabal, Phys. Rev. Lett. **55**, 845 (1985).
[34]K. E. Smith and S. D. Kevan, Phys. Rev. Lett. **64**, 567 (1990).
[35]J. E. Reutt, Y. J. Chabal, and S. B. Christman, Phys. Rev. B **38**, 3112 (1988).